ORIGINAL PAPER

Impacts of Spectral Characteristics of Dissolved Organic Matter on Methyl Mercury Contents in Permafrost Wetlands, Northeast China

Fan Sun[1,2] · Meijie Zheng[1] · Shan Jiang[1] · Qiang Guan[1] · Zhongsheng Zhang[1] · Dongmei Zheng[2]

Abstract

Dissolved organic matter (DOM) plays an important role in promoting or suppressing methylmercury (MeHg) production in wetlands. However, in the context of climate warming, the regulatory mechanism of DOM composition and molecular structure changes in permafrost wetland soil on mercury methylation remains unclear. In this study, we analyzed the distribution characteristics of mercury and methylmercury in permafrost wetland soils in the Greater Khingan Mountains (GKM), and elucidated the driving mechanism of mercury methylation by basic physical and chemical properties and DOM spectral characteristics of soils. The results showed that the mean value of total mercury in the permafrost wetlands of the GKM was 111 ng·g^{-1}, the mean value of methylmercury was 5.69 ng·g^{-1}, and the mean percentage of methylmercury was 6.16%. Hg and MeHg concentrations showed different vertical distribution patterns in the four wetlands, with Hg and MeHg concentrations in both scrub and moss wetlands showing a decreasing trend with soil deepening, but herb and forest wetlands did not satisfy this pattern. Soil warming, associated with the decomposition and mineralization of Soil Organic Matter (SOM), induces an elevation in Dissolved Organic Matter (DOM) content, subsequently contributing to increased levels of mercury methylation and an upswing in methylmercury output. Throughout this process, the spectral properties of DOM play a pivotal role in regulating Hg methylation, with the input of plant sources following closely behind. The content of MeHg in the soil is minimally influenced by the mercury content in the soil.

Keywords The Greater Khingan Mountains · Methylmercury · Dissolved organic matter · Spectral characteristics

1 Introduction

Mercury (Hg) is considered to be a global pollutant due to its long-range transport via the atmosphere, transformation between various species, and biomagnification along food webs (Selin et al., 2009). Hg biological cycles have been a subject of significant scientific interest over the past decades (Sun et al. 2017). Wetland plays a crucial role in controlling the distinctive biogeochemical cycling of Hg (Adediran et al., 2019; Beckers et al. 2019), which usually serves as Hg sink and methylmercury (MeHg) source to the ambient. The retention rate of mercury in peatlands has been reported to be 20 mg·m^{-2}, which is much higher than that in forest topsoil (1 mg·m^{-2}). Meanwhile, the anaerobic and organic-matter-rich soil conditions of wetlands favor MeHg production by microbes (Driscoll et al. 2007), which are about $26 \sim 79$ times higher than those in upland areas. According to projections from the Intergovernmental Panel on Climate Change's (IPCC) Fifth Assessment Report, there has been an approximate 0.85 °C increase in global temperatures over the past century. The Great Khingan Mountains (GKM) area in Northeast China, characterized by its swampy and permafrost wetlands, has experienced a significant reduction in permafrost coverage by about 35% due to recent warming trends (Jin et al. 2006). This gradual thawing of permafrost could lead to substantial releases of mercury into the ecosystem, posing serious risks to environmental health.

Beyond the immediate emissions of mercury from permafrost zones, both the influx and outflow of mercury, along with its methylation process, are intricately linked to types of vegetation. Recent investigations have underscored the critical role of mercury's dry deposition within terrestrial

✉ Zhongsheng Zhang
  zzslycn@iga.ac.cn

1 Northeast Institute of Geography and Agroecology, Chinese
   Academy of Sciences, Changchun 130102, China

2 Shenyang University College of Environmental,
   Shenyang 110044, China

ecosystems. In particular, the absorption of atmospheric Hg0 by plant life plays a pivotal role in the significant accumulation of mercury in soil (Jiskra et al. 2015; Wang et al. 2016; Schuster et al., 2018). The research findings of Feng et al. Hg concentration in surface soil is highly correlated to vegetation related factors (He et al., 2015). This suggests that the Hg input driven by vegetation activities being the main factor causing the observed Hg pool size. Meanwhile, climate is the main driver for vegetation distribution globally (Ding et al. 2017; Piao et al. 2018). Xue et al. showed that permafrost degradation caused by climate warming is a key factor affecting plant community distribution in GKM wetland (Xue et al., 2021). In the context of global warming, a significant shift is expected, where herbaceous and shrubby wetlands will encroach upon moss-dominated wetlands on a large scale. This phenomenon is particularly pronounced in high-latitude regions, where the invasion by shrub wetlands stands out the most. This trend underscores the importance of investigating how mercury levels fluctuate across wetlands with varying types of vegetation cover.

There is covariation between carbon and mercury in soil, especially dissolved organic matter (DOM) change, which is one of the main controlling factors of mercury methylation in permafrosr soil. MeHg production in wetlands is proven greatly affected by DOM (Chen et al. 2020; Gerbig et al. 2012), which usually affects Hg cycle greatly, not only by stimulating MeHg synthesis or introducing demethylation (Ullrich et al. 2001; Frohne et al. 2012), but also by forming stable Hg complexes with reduced sulfur groups such as thiols (Eagles et al., 2014). DOM is usually easily assimilated by microbes and then enhances Hg methylation (Abdelhafiz et al. 2023; Gerbig et al. 2012; Vrivens et al., 2014; Wang et al. 2021). Multiple studies reported that higher levels of DOM increased Hg bioavailability, methylation, and bioaccumulation (Lin et al. 2014; Wang et al. 2021), where labile fractions are relatively high and readily biodegradable; it may enhance methylation by stimulating microbial growth (Patriarca et al. 2021).

Therefore, based on the above understanding, we propose two hypotheses: (1) With global warming, the invasion of herbaceous and scrub wetlands into permafrost wetlands will significantly change the distribution pattern of Hg and MeHg in wetland soils; (2) In this process, DOM content and its structural characteristics will contribute to the process of Hg methylation.

2 Methods and Materials

2.1 Study Area

The Great Khingan Mountains (GKM), boasting the highest concentration of wetlands in China, are situated on the northeastern periphery of the country (40°59′–53°33′ N, 115°50′–130°51′E; Fig. 1). The region experiences a cold and prolonged winter, coupled with a cool and brief summer, resulting in a substantial diurnal temperature variation. The annual average temperature stands at -2.8 °C, with extreme temperatures plummeting to -50 °C. This climate is characterized as a cold temperate continental monsoon climate (Gao et al. 2016). Predominant natural features encompass forests and swamps. The swamps primarily manifest at the valley bottoms across the GKM and on platforms in the North, underlain by permafrost. The permafrost region of the GKM can be delineated into continuous permafrost and segregated permafrost areas, encompassing a total area of approximately 1.12×105 km^2 (Xin et al. 2023).

2.2 Sample Collection and Treatment

Soil profiles were collected at 14 sites surrounding the GKM (122°00'E~125°00'E, 50°10'N~53°33'N) permafrost Wetlands in September 2021. Sample sites were categorized into four types according to the predominant plant covers, which were herb (Hc, $n=5$), shrub (Sc, $n=5$), forest (Fc, $n=2$), and moss (Mc, $n=2$), according to the predominant vegetation. After removing the surface litter, samples of the vertical profile of the soil were taken from top to bottom (each sample had a thickness of 5 cm). The collection depth was 40 cm. The soil samples were smashed with a wooden hammer, allowed to air dry at room temperature (20~25°C), and sieved through a 2 mm sieve. The filtrates were stored at -4 °C before analysis or further treatments.

2.3 Analytical Methods

Total Hg (THg) and methylmercury (MeHg) in soil samples were analyzed as described in Zhang et al. (Zhang et al. 2020). For the quantification of THg in the soil, 0.2 g of the soil sample was meticulously weighed and subjected to digestion with 10mL of HNO^3 and 2.5mL of H$_2$SO$_4$. Following the cooling process, two drops of KMnO$_4$ indicator were introduced to facilitate complete reaction over a one-hour period. The reacted solution was then transferred to a colorimetric tube, and the volume was adjusted to 50 ml with HCl (concentration ratio of 5%) for subsequent measurement. To determine MeHg in the soil, 1.0 g of the soil sample was immersed in 10 mL of HCl (6 N) and allowed to stand overnight. Subsequently, MeHg was extracted
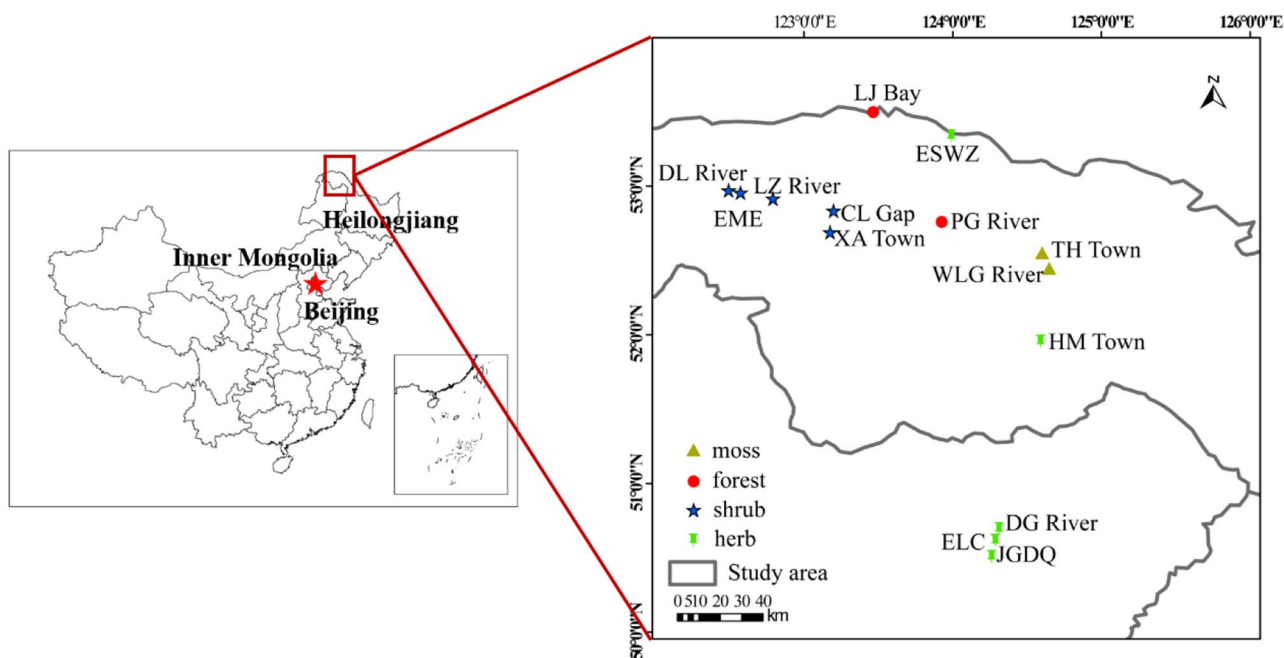
Fig. 1 The study area is in the Greater Khingan Mountains, northeast China. TH Town, Tahe Town; WLG River, Walagan River; LJ Bay, Longjiang Bay; PG River, Pangu River; DL River, Dalin River; LZ River, Laozao River; EME, Eermu; CL Gap, Chulong Gap; XA Town, Xingan Town; ESWZ, Ershiwuzhan Site; DG River, Dagen River; ELC, Elunchun autonomous banner; JGDQ, Jiagedaqi

twice consecutively with 5 mL of CH_2Cl_2, with the separated CH_2Cl_2 transferred to a heart-shaped bottle. Following the addition of 5.0 mL of deionized water, the removal of CH_2Cl_2 was accomplished by rotary evaporation, leaving MeHg in the deionized water. The oxidation process involved the addition of a brominating agent (comprising an equal volume of KBr and $KBrO_3$), followed by reduction with NH_4HCO_3 to convert Hg^{2+} to Hg^0. The final determination was carried out using CVAFS instrument (Haiguang, Beijing).

Soil total carbon (TC) and total nitrogen (TN) were determined by an elemental analyzer (Elementar Vario Macro cube); soil soluble organic carbon (DOC) was determined by a total organic carbon analyzer (TOC-2000, Gangdong, Tianjin, China), and the data deviations (RSD) of the measurements of all parallel samples were less than 5%.

For quality control, standard materials were used to test the precision and accuracy of THg (Reference material number: GBW07978) and MeHg (Reference material number: SCQC-122) determination. The recoveries were 95~103% and 92–105%, respectively.

2.4 The UV–Vis and Fluorescence Spectrum of DOM

The UV–Vis spectrum (UV–2550, Shimadzu, Japan) and fluorescence spectrum (F–4700, Hitachi, Japan) were conducted to characterize the molecular features of DOM. For UV–Vis analysis, using deionized water as a blank, the absorption spectrum from 200 nm to 800 nm was measured, and the scanning speed was set to 1 nm. DOM indices, defined as adsorption at specific wave or absorbance ratios at different bands including $SUVA_{254}$, $SUVA_{260}$, A250/A365, A465/A665, A253/A203 and A240/A420 were applied to characterize the source, structure, and composition of DOM. Detailed information can be found in Table S1.

For fluorescence analysis, first, all samples are diluted with 0.1 $mol·L^{-1}$ phosphate buffers (PH = 7) according to the DOC concentration of the sample. The final DOC content was set to approximately 8 $mg·L^{-1}$. Fluorescence EEM spectroscopy was performed for each sample at room temperature with excitation and emission wavelength ranges of 250–450 and 300–600, respectively, at 2 nm intervals, and scanning speed of 1200 nm/min. All spectral corrections were performed using parallel factor analysis (PARAFAC) in the Matlab software environment (Schaefer et al., 2014). Three fluorescence indexes (FI, HIX, BIX) were used to characterize the source and humification degree of DOM. Detailed information can be found in Table S1.

2.5 Statistical Analysis

The ANOVA analysis was performed to make comparisons of THg, MeHg, and %MeHg among samples from

different wetlands. The correlation analysis was used to decipher relations between THg, MeHg, and %MeHg and multiple factors. The principal component analysis was used to group dimensionality reduction for multiple control factors. The random forest analysis was used to rank the factors controlling mercury methylation. We established a structural equation model to reveal the direct and indirect effects of DOM spectral signature on Hg methylation. The path coefficients were used to reflect the strengths of direct and indirect effects. All statistical analysis was carried out using the R (Version 4.2.1) software.

3 Results

3.1 THg and MeHg Contents in Wetland Soils of the GKM

The average values of THg and MeHg were 111.1 ng·g^{-1} and 5.69 ng·g^{-1}, respectively, with a range of 32.3 ng·g^{-1} to 278.3ng·g^{-1}, 0.11 ng·g^{-1} to 17.6 ng·g^{-1}, respectively (Fig. 2). The average %MeHg was 6.16%, with an average of 0.15–22.18%. THg and MeHg were 115.8 ng·g^{-1} and 5.42 ng·g^{-1} in Hc, 87.29 ng·g^{-1} and 9.69 ng·g^{-1} in Mc, 106.6 ng·g^{-1} and 2.54 ng·g^{-1} in Sc, and 93.19 ng·g^{-1} and 5.58 ng·g^{-1} in Fc, respectively, depending on the type of wetland. Between groups, there are significant difference in THg, MeHg, and %MeHg ($p < 0.05$). Overall, THg contents ranked as Hc > Sc > Fc > Mc, MeHg contents changed
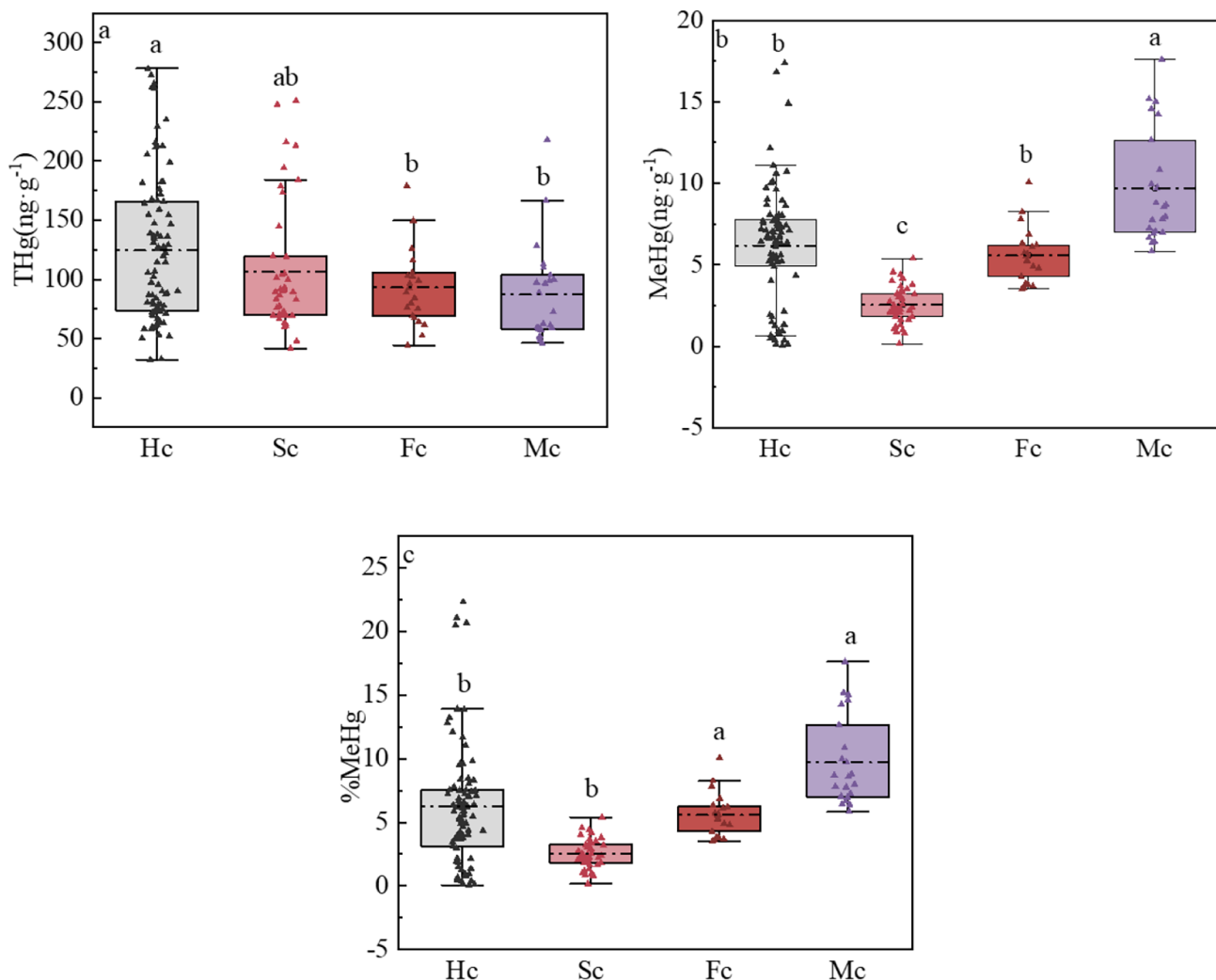

Fig. 2 Comparison of total mercury (THg), methyl mercury (MeHg), and rate of methylmercury formation (%MeHg) among different wetlands. (Hc stands for herb wetland, Sc stands for shrub wetland, Fc stands for forest wetland, Mc stands for moss wetland)

in the order of Mc > Hc > Fc > Sc, and %MeHg ranked as Mc > Hc > Fc > Sc.

3.2 Profile Distribution of THg and MeHg in Wetland Soils

In various wetland ecosystems, concentrations of THg, MeHg, and DOC exhibit variability across soil profiles (Fig S1-S4). Generally, within Hc, Sc, and Mc environments, THg levels show a decreasing trend with increased soil depth, with peak concentrations typically found in the topmost soil strata at the majority of test sites. Conversely, in Fc ecosystems, the greatest THg concentrations are identified in the lowermost soil layers. Across these wetland types, MeHg levels remain relatively stable, showing no marked variation with soil depth progression. In Hc, Mc, and Fc settings, DOC concentrations diminish as soil depth increases, with the highest levels present at the soil surface.

3.3 Spectral Characteristics of DOM

For DOM spectral characteristics, Fc exhibited the highest SUVA254 and SUVA260 values, while Mc demonstrated the highest A240/A420, A250/A365, and A465/A665 ratios. Hc, on the other hand, displayed the highest A253/A203 ratio. Notably, all A250/A365 ratios in Mc exceeded 3.5, suggesting a predominance of fulvic acid with comparatively low molecular weight in the DOM. Additionally, the low A253/A203 values observed in GKM implied a simple

material composition in this area, primarily comprising fatty chains.

Four components were extracted from the EEMs dataset by PARAFAC analysis. C1 (Ex/Em = 240, 260, 310/410; Fig. 3(1) and C2 (Ex/Em = 200/370; Fig. 3(2) belonged to the UV-like fullerene fluorescence (Peak A), which is mainly derived from degradation by wetland plants and is commonly used as an indicator of exogenous inputs. The C3 (Ex/Em = 230, 280/402; Fig. 3(4) belongs to fulvic acid like in visible light fluorescence (peak C) (He et al., 2015). The C4 (Ex/Em = 270, 310/470; Fig. 3(4) belongs to humic acid, which contains various functional groups capable of effectively adsorbing heavy metals (Liu 2022).

The FI values, which ranged from 1.4 to 1.9 across all wetlands (Fig. 3), suggest that there may be contributions from both external sources and microbial decomposition to DOM. All BIX values were below 0.8 in all samples, indicating a low biological index of decomposition. All HIX values were less than 4, suggesting a relatively low degree of humification of DOM in the GKM region.

3.4 Correlation Analysis and Principal Component Analysis

THg exhibits a positive correlation with TC, TN, DOC, and A240/A420 at a significant level. Conversely, it shows a negative correlation with BIX and A253/A203 at a significance level of $p < 0.01$. In contrast, MeHg concentration demonstrates positive correlations with DOC, TN, TC, A240/A420, A250/A365, and A465/A665 at a significant

Fig. 3 Excitation-emission matrices (EEMs) of soil dissolved organic matter (DOM) from the GKM. (Ex and Em represent the excitation matrix and emission matrix)
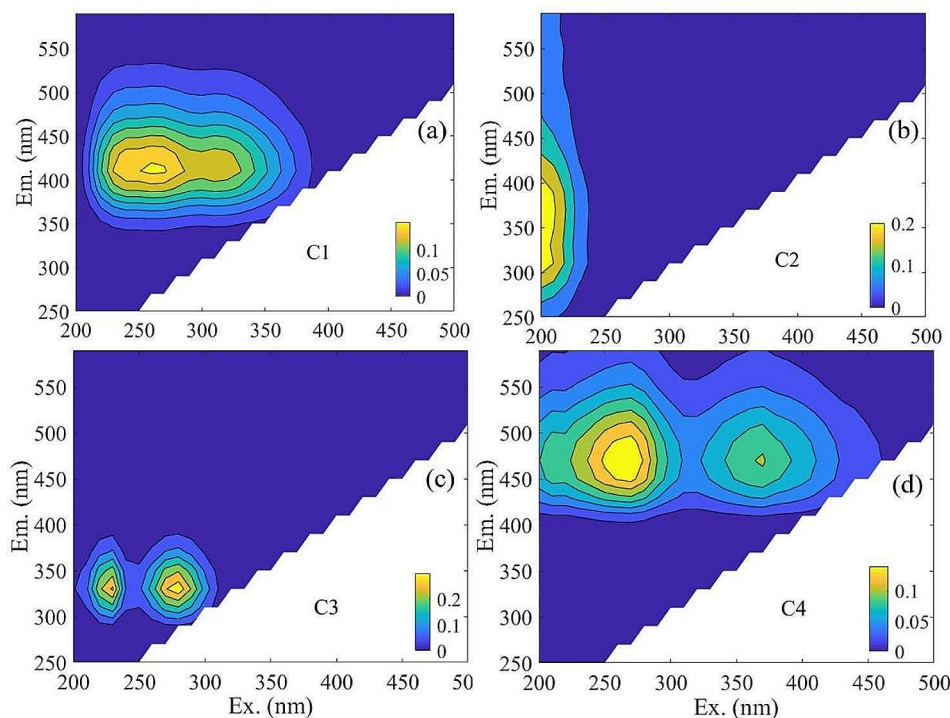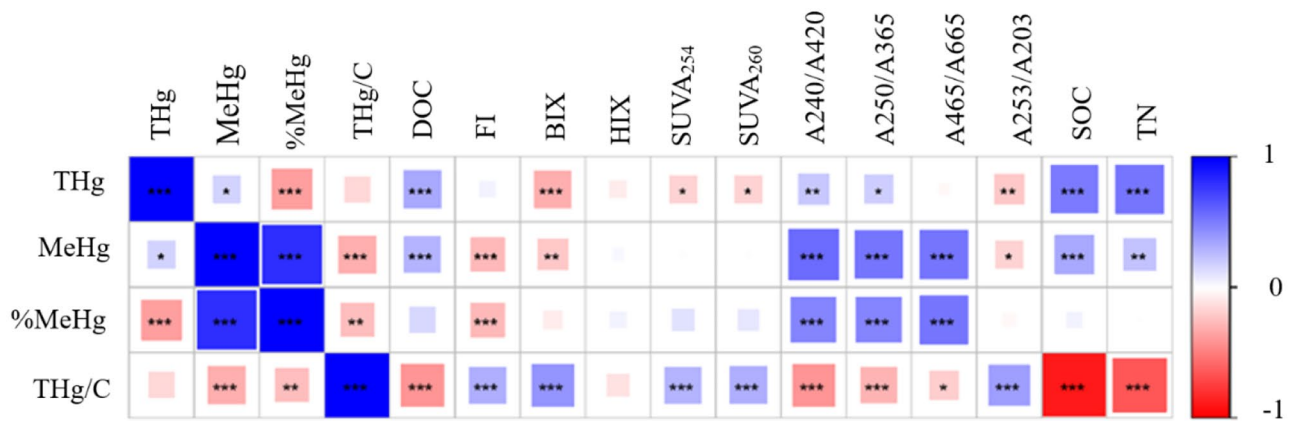
Fig. 4 Relationships between total mercury (THg), methylmercury (MeHg), rate of methylmercury formation (%MeHg), Hg/C and environmental factors. Square colors represented negative or positive relationships while square size meant the absolute values, the blank meant no significant correlations were observed. $^{***}p<0.001$; $^{**}p<0.01$; $^{*}p<0.05$. DOC, dissolved organic carbon; SOC, total carbon; TN, total nitrogen; SUVA$_{254}$, degree of humification of DOM; SUVA$_{260}$, hydro-

phobic components of DOM; A240/A420, intermolecular condensation of DOM; A250/A365, aromaticity index and Relative molecular mass; A465/A665, extent of polymerization of Benzene ring; A253/A203, complexity of material structure; FI, source of humus; HIX, humification process of DOM; BIX, endogenous origin is contribution of DOM
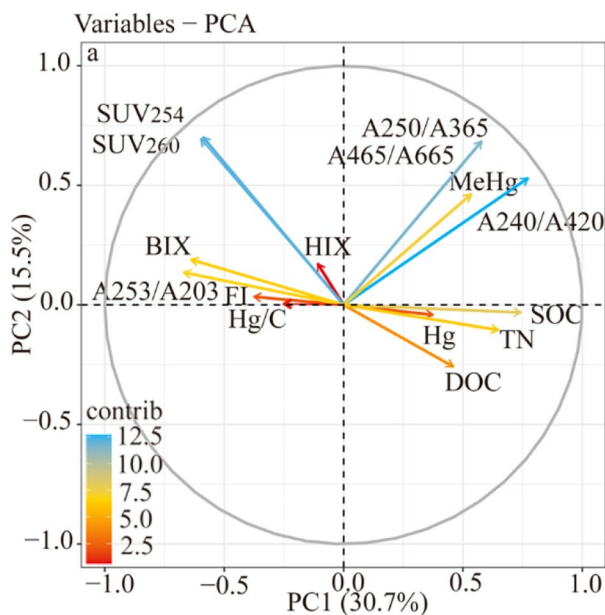

Fig. 5 PCA analysis for deciphering relations between total mercury (THg), methylmercury (MeHg) and multiple environmental factors. DOC, dissolved organic carbon; SOC, total carbon; TN, total nitrogen; SUVA$_{254}$, degree of humification of DOM; SUVA$_{260}$, hydrophobic components of DOM; A240/A420, intermolecular condensation of

DOM; A250/A365, aromaticity index and Relative molecular mass; A465/A665, extent of polymerization of Benzene ring; A253/A203, complexity of material structure; FI, source of humus; HIX, humification process of DOM; BIX, endogenous origin is contribution of DOM
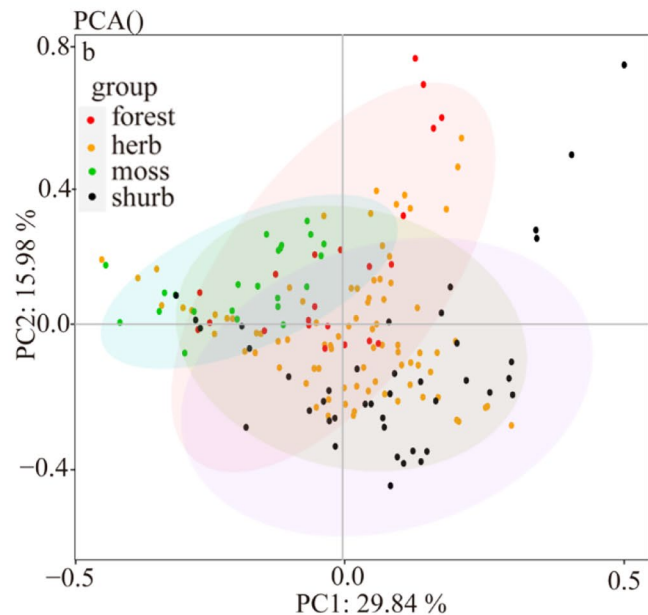
level, while exhibiting negative correlations with FI, BIX, and A253/A203 at a significance level of $p<0.01$. Furthermore, the percentage of MeHg is negatively correlated with FI at a significance level of $p<0.001$, while displaying positive correlations with A240/A420, A250/A365, and A465/A665 at a significance level of $P<0.001$ (Fig. 4).

The PCA analysis revealed that the first two principal components collectively accounted for 46.2% of the total variance (Fig. 5). The PC1, which explained 30.7% of the total variance, was indicative of the potential influence of vegetation on both THg and MeHg, as evidenced by the positive loadings of TC and TN on PC1 (Wang et al., 2019a).

Fig. 6 The random forest approach was used to calculate potential drivers of variation affecting mercury methylation. $^{***}p < 0.001$; $^{**}p < 0.01$; $^{*}p < 0.05$. where structural is the value of the first principal component after principal component analysis of A240/A420, A250/A365, and A465/A665, humification is the value of the first principal component after principal component analysis of SUVA$_{254}$, BIX, and A253/A203. DOC, dissolved organic carbon; SOC, total carbon; TN, total nitrogen; THg, total mercury; MeHg, methylmercury
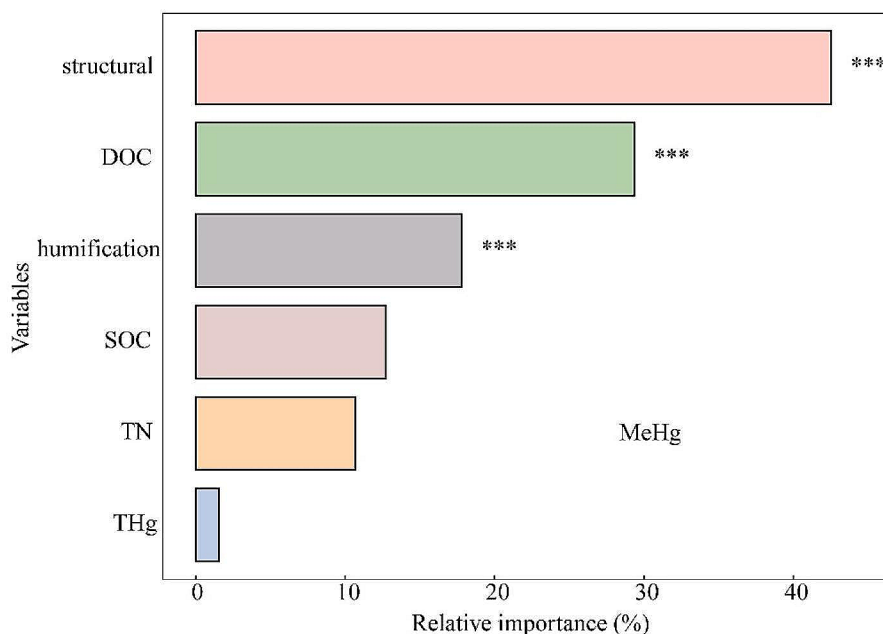

Table 1 Comparison of total mercury (THg), methylmercury (MeHg) and rate of methylmercury formation (%MeHg) between the Great Khingan Mountains (GKM) region and other sites

Locations	THg(ng·g^{-1})	MeHg(ng·g^{-1})	%MeHg	References
Arctic Fennoscandian	13～210	0.17～0.78	0.48～6.1	Hudelson et al. 2020
Tibetan Plateau	14.8	——	——	Sun et al. 2017
Northwestern Ontario	162	0.6±0.6	——	Mailman et al., 2005
Penobscot River marshes	100	2～50	2～8	Gilmour et al. 2018
Canadian boreal	117	0.31	0.23	Huang et al., 2023
Moor in Cornwallis Island	5.05～51.75	0.02～0.54	0.1～0.6	Hudelson et al. 2020
Arctic surface sediments	24.30	0.11	0.03～0.9	Lin et al. 2014
Arctic Ny-Ålesund	21～48	0.65～1.08	2	Jiang et al. 2011
GKM	111.1	5.69	6.16	The present work

The PC2, explaining 15.5% of the total variance, suggested the impact of DOM molecular characteristics on MeHg production. This inference is supported by all spectral parameters displaying positive loadings on PC2, with SUVA254, representing the degree of DOM humification, exhibiting the largest positive loading. The humification level of DOM is known to facilitate Hg methylation (Ouellet et al. 2009). The PCA analysis corroborated the associations between THg, MeHg, %MeHg, DOM spectral attributes, and environmental factors as indicated in the correlation analysis.

3.5 Random Forest Analysis

Random forest analysis showed that the structural characteristics of DOM had the greatest effect on methylmercury content, followed by the effect of DOC, and thirdly the effect of the degree of DOM humification, and all of them reached a significant level (Fig. 6). The result was consistent with the study of Abdelhafiz et al. (Abdelhafiz et al. 2023).

TC and TN were also the main drivers affecting MeHg, indicating that the plant-derived SOC played important roles in MeHg production (Xin et al. 2023). THg are less important for MeHg, indicating that MeHg in permafrost wetlands in the GKM mainly comes from exogenous input, and the historical load and mineralization capacity of the soil itself has less influence on MeHg production (Liu et al. 2014).

4 Discussion

The THg content in the permafrost wetland soils of the GKM is approximately 2.7 times higher than the Chinese soil background value of 40 ng·g^{-1}, suggesting that the GKM wetlands function as a regional mercury sink. Moreover, THg and MeHg levels in the study area notably surpass those observed in remote regions across Europe and the Arctic regions (Table 1). For instance, the average THg content in Northwestern Ontario stands at 162 ng·g^{-1}, with the

average MeHg content at a mere 0.6 ± 0.6 ng·g^{-1}. The THg concentrations in the GKM are six times higher than those found on the Tibetan Plateau, a disparity likely attributed to increased anthropogenic activities such as coal consumption and industrial emissions in regions like Heilongjiang and Inner Mongolia. In particular, the extensive coal combustion in the GKM regions, occurring for more than 180 days per year, leads to significantly elevated atmospheric mercury concentrations in the area. A prior study conducted at various urban sites in Changchun, northeastern China, spanning from July 1999 to July 2000, revealed annual mean atmospheric mercury concentrations ranging from 11.7 to 18.4 ng·m^{-3}, one order of magnitude higher than the background concentrations in the Northern Hemisphere (Fichot et al., 2012), which finally deposited and cause high Hg pollution (Tomiyasu et al. 2020). THg content of the Arctic Fennoscandian permafrost varied between 13 ng·g^{-1} to 210 ng·g^{-1}, which is similar to the GKM permafrost region. However, the proportion of MeHg to THg was lower in the Arctic Fennoscandian permafrost compared to the GKM permafrost region. This could be attributed to the cold climate and limited availability of bioavailable carbons in the Arctic, creating an unfavorable soil environment for the survival of certain methylating microorganisms like sulfate-reducing bacteria (Shao et al. 2012).

From the correlation analysis, it can be seen that there is a significant positive correlation between methylmercury and DOC, which suggests that the higher the level of DOC, the higher the degree of mercury methylation in wetland ecosystems. It has been shown that DOC degradation and mercury methylation are coupled in anaerobic environments (Liu et al. 2016; Yang et al. 2016). The ability to degrade DOC can influence the activity and distribution of soil microorganisms, which in turn can affect net concentrations of MeHg (Christensen et al. 2018). For example, microbial communities regulated by DOC may influence MeHg production. DOC levels have been reported to correlate significantly with the relative abundance of microbial taxa such as Geobacteriaceae, a key taxon involved in MeHg formation (Wei et al. 2020). Although DOC plays an important role in MeHg production, it seems to be masked in some cases. In the tundra wetlands of the GKM, there was no significant correlation between %MeHg and DOC, probably because %MeHg was related not only to MeHg concentrations but also to total Hg concentrations (Drott et al. 2008).

The generation and degradation processes of DOM result in the formation of numerous functional groups. These groups play a pivotal role in regulating the mobility, bioavailability, and toxicity of mercury by influencing its adsorption and complexation with DOM (Bai et al. 2018). Consequently, it is imperative to investigate the impact of mercury methylation on the spectral characteristics of

DOM. PCA analysis partitioned the spectral features into two components. A250/A365, A240/A420, and A465/A665, indicative of the structural characteristics of DOM, reside on the positive load of PC1. Conversely, BIX and SUVA$_{254}$, reflecting the degree of DOM humification, are positioned on the positive load of PC2. The minimal angle observed between Hg, FI, and BIX implies that mercury can form bonds with aromatic and humic-like components. The negative correlation observed between MeHg and FI as well as BIX suggests that exogenous DOM fractions are involved in complexation with Hg. This implies that Hg forms complexes with aromatic and humic fractions, which contributes to the immobilization of mercury and subsequently decreases its bioavailability. The complexation of Hg with these specific DOM components can have significant implications for the environmental fate and toxicity of mercury. The minimal angle observed between MeHg and spectral features A240/A420 and A250/A365 suggests that at higher molecular weights, DOM facilitates the methylation of Hg^{2+} (Mitchell and Gilmour 2008). This phenomenon can be attributed to two main factors. Firstly, the hydrophobic acid fraction of DOM, including humic and fulvic acid fractions, is significantly higher than the low molecular weight hydrophilic acid fraction (Ravichandran 2004). This higher content of reduced sulfur (comprising polysulfide, sulfide, and mercaptan groups) in the hydrophobic acid fraction, especially in the presence of strongly complexed thiols, promotes the methylation of mercury (Schaefer et al. 2011). In comparison to oxygen ligands, thiols, and disulfides are favored sites for the complexation of Hg with DOM (Mitchell and Gilmour 2008). Additionally, the aromatic groups within DOM play a crucial role in promoting the release of insoluble mercury, thereby facilitating and enhancing the methylation of mercury. This underscores the significance of specific functional groups in DOM that contribute to the complexation and subsequent transformation of mercury species in the environment.

Level of mercury methylation dependent on THg/C ratios owing to the dominant roles of strong binding sites (e.g., thiol) at low THg/C and weak binding sites (e.g., oxygen-containing functional groups including carboxyl and hydroxyl) at high THg/C. Therefore, various THg/C concentration ratios were used to reflect the different binding strengths of DOM to Hg^{2+} in this study (Wang et al. 2022). Figure 7 shows a positive correlation between THg/C, FI and BIX, this suggests that the higher the degree of humification of DOM and the higher the organic matter content, the stronger the methylation of mercury, possibly through stimulation of microbial activities via the availability of abundant electron donors (Barkay and Gu 2022). We can reasonably speculate that higher total carbon can Increase mercury levels in the soil by increasing Hg adsorption onto
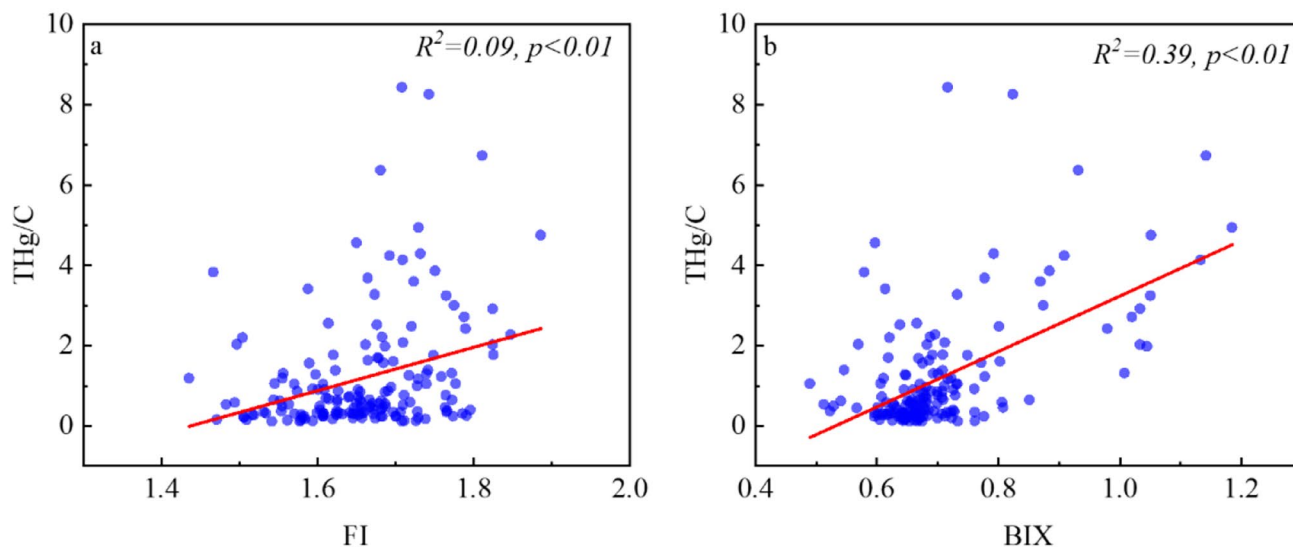
Fig. 7 Correlation analysis between THg/C and FI and BIX. (THg/C were used to reflect the different binding strengths of DOM to Hg^{2+}; FI, source of humus; BIX, endogenous origin is contribution of DOM)

sediment organic matter, particularly the reduced sulfur groups in organic matter, which in turn promotes soil Hg methylation (Skyllberg et al. 2003). Both FI and BIX values indicate that soil DOM in GKM is dominated by exogenous inputs, most of which come from the transformation of organic matter. Theoretically, exogenously imported DOM has more hydrophobic components and higher molecular weights than endogenously imported DOM, which may provide more binding sites, especially sulfate groups such as thiols (Jiang et al. 2018). Humic-type DOM exhibits higher binding capacity. Previous studies have reported that the hydrophobic components of DOM, especially humic molecules, have higher content of reduced sulfur (e.g., sulfides and thiols), resulting in a preferential affinity for mercury, which is consistent with the findings of this paper.

Interestingly, MeHg levels and the percentage of MeHg were found to be highest in the wetlands of the Mack area and lowest in the Sc wetlands. One plausible explanation for this variation is that the absence of a root and cuticle layer system in the mosses makes their cell walls easily accessible to mercury ions, leading to extensive absorption across the entire surface (Adediran et al., 2019). Mosses have the capacity to accumulate heavy metals through both intracellular and extracellular processes. These distinctive characteristics render them ideal biomonitors for atmospheric pollutants, including mercury (Li et al., 2020). Certainly, the moist environment and the evergreen nature of moss contribute to the accumulation of organic matter, creating favorable conditions for the methylation of mercury (Wang et al. 2019b). Studies have reported a strong positive relationship between soil mercury emission and methylmercury production with temperature (Ci et al.

2018). Climate warming can impact soil conditions, leading to lower water content, higher bulk density, and increased pH, all of which contribute to enhanced soil organic matter decomposition and mercury emissions. In cold regions, where soil organic carbon is more susceptible to climate change due to microbial thermal adaptation, increased temperatures may result in substantial carbon decomposition, leading to higher mercury release (Karhu et al. 2014; Mu et al. 2016). Additionally, the northward expansion of moss or forest into peatlands, driven by climate warming, can introduce more biomass into soils. Considering these factors, it becomes crucial to focus on the generation of mercury and the transformation of methylmercury in the GKM as climate warming progresses. Monitoring these processes is essential for understanding the potential impacts on environmental mercury levels and associated risks.

The structural equation model (SEM) was established to reveal the direct and indirect effects of TN, SOC, DOC, and structural, humification, and THg on MeHg (Fig. 8). It is clear that TN and SOC are the main factors influencing the Hg content, suggests that Hg in the GKM is mainly derived from inputs from plant sources. MeHg in soil is mainly influenced by a combination of structural characteristics and the degree of humification in DOM. They not only control the binding sites between Hg^{2+} and different functional groups but also influence microbial activities and species, thereby controlling the methylation of mercury in soil. Figure 8 shows that THg has less effect on MeHg, this might imply methylmercury in the Greater Khingan Mountains is mainly imported from external sources, this is consistent with the previous conclusion. Based on the SEM model results, it is inferred that the MeHg content in GKM is mainly affected
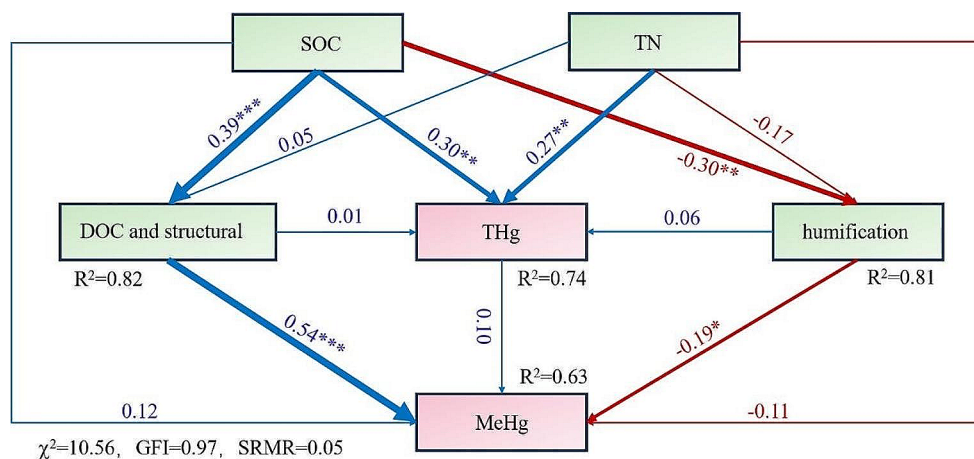
Fig. 8 The total effects of multiple factors on mercury methylation. (Blue represents positive effects, red represents negative effects; *Significant at the 0.05 probability level; $^{***}p < 0.001$; $^{**}p < 0.01$; $^{*}p < 0.05$) where DOC and structural is the value of the first principal component after principal component analysis of DOC, A240/A420, A250/A365, and A465/A665, humification is the value of the first principal component after principal component analysis of SUVA$_{254}$, BIX, and A253/A203. DOC, dissolved organic carbon; SOC, total carbon; TN, total nitrogen; THg, total mercury; MeHg, methylmercury

by the DOM spectral characteristics, and has little relationship with the own mercury accumulation.

5 Conclusions

Our research framework unveiled the interplay among soil mercury methylation, Dissolved Organic Matter (DOM), and its spectral characteristics in the peatlands of the high-latitude permafrost region in Northeast China. Our results not only highlighted the promoting influence of DOM spectral characteristics on mercury methylation in peatlands with diverse vegetation types but also indicated that the ongoing permafrost thaw, coupled with changes in surface vegetation processes in the current scenario of climate warming, will significantly impact regional mercury cycling. Specifically, the widespread transition from mosses to grasses and shrubs due to climate warming may potentially augment the influx of mercury from vegetation sources into the soil. Simultaneously, soil warming, inherent in the decomposition and mineralization of Soil Organic Matter (SOM), results in an upsurge in DOM content, subsequently leading to heightened levels of mercury methylation and an increase in the flux of methylmercury output. This presents a potential ecological risk to the regional ecosystem, especially in the future. Hence, emphasis should be placed on this aspect.

Declarations

Ethics Approval This work does not include any animal or patient experiments, so no ethics approval is needed. Soil sample collection was approved by the local government.

Consent to Participate Not applicable.

Consent for Publication Not applicable.

Conflict of Interest The authors declare no competing interests.

References

Abdelhafiz MA, Liu J, Jiang T, Pu Q, Aslam MW, Zhang K, Feng X (2023) DOM influences hg methylation in paddy soils across a hg contamination gradient. Environ Pollut 322:121237. https://doi.org/10.1016/j.envpol.2023.121237

Adediran GA, Liem-Nguyen V, Song Y, Schaefer JK, Skyllberg U, Bjorn E (2019) Microbial biosynthesis of thiol compounds: implications for speciation, cellular uptake, and methylation of hg (II). Environ Sci Technol 53:8187–8196. https://doi.org/10.1021/acs.est.9b01502

Bai H, Jiang Z, He M, Ye B, Wei S (2018) Relating Cd^{2+} binding by humic acids to molecular weight: a modeling and spectroscopic study. J Environ Sci 70:154–165. https://doi.org/10.1016/j.jes.2017.11.028

Barkay T, Gu B (2022) Demethylation—the other side of the mercury methylation coin: a critical review. ACS Environ Au 2:77–97. https://doi.org/10.1021/acsenvironau.1c00022

Beckers F, Awad YM, Briyuan J, Abrigata J, Mothes S, Tsang DC, OK S Y, Rinklebe J (2019) Impact of biochar on mobilization, methylation, and methylation of mercury under dynamic redox conditions in a contaminated floodplain soil. Environ Int 127:276–290. https://doi.org/10.1016/j.envint.2019.03.040

Chen Q, Jia R, Li L, Qu D (2020) Effects of high concentrations of sulfate on dissolved organic matter in paddy soils revealed by excitation-emission matrix analyzing. Chemosphere 249:126207. https://doi.org/10.1016/j.chemosphere.2020.126207

Christensen GA, Somenahally AC, Moberly JG et al (2018) Carbon amendments alter microbial community structure and net mercury methylation potential in sediments. Appl Environ Microbiol 84:e01049–e01017. https://doi.org/10.1128/AEM.01049-17

Ci Z, Peng F, Xue X, Zhang X (2018) Temperature sensitivity of gaseous elemental mercury in the active layer of the Qinghai-Tibet Plateau permafrost. Environ Pollut 238:508–515. https://doi.org/10.1016/j.envpol.2018.02.085

Ding JZ, Chen LY, Ji CJ, Hugelius G, Li YN, Liu L, Qin SQ, Zhang BB, Yang GB, Li F, Fang K, Chen YL, Peng YF, Zhao X, He HL, Smith P, Fang JY, Yang YH (2017) Decadal soil carbon accumulation across Tibetan permafrost regions. Nat Geosci 10:420–424

Driscoll CT, Han YJ, Chen CY, Evers DC, Lambert KF, Holsen TM, Kamman NC, Munson RK (2007) Mercury contamination in forest and freshwater ecosystems in the northeastern United States. Bioscience 57:17–28. https://doi.org/10.1641/B570106

Drott A, Lambertsson L, Björn E, Skyllberg U (2008) Do potential methylation rates reflect accumulated methyl mercury in contaminated sediments? Environ Sci Technol 42:153–158. https://doi.org/10.1021/es0715851

Eagles-Smith CA, Ackerman JT (2014) Mercury bioaccumulation in estuarine wetland fishes: evaluating habitats and risk to coastal wildlife. Environ Pollut 193:147–155. https://doi.org/10.1016/j.envpol.2014.06.015

Fichot CG, Benner R (2012) The spectral slope coefficient of chromophoric dissolved organic matter (S275–295) as a tracer of terrigenous dissolved organic carbon in river-influenced ocean margins. Limnol Oceanogr 57:1453–1466. https://doi.org/10.4319/lo.2012.57.5.1453

Frohne T, Rinklebe J, Langer U, Du Laing G, Mothes S, Wennrich R (2012) Biogeochemical factors affecting mercury methylation rate in two contaminated floodplain soils. Biogeosciences 9:493–507. https://doi.org/10.5194/bg-9-493-2012

Gao Y, Zhao H, Gao F, Zhu H, Qu H, Zhao F (2016) Climate change trend in future and its influence on wetlands in the Greater Khingan Mountains. J Glaciol Geocryol 38:47–56

Gerbig CA, Ryan JN, Aiken GR (2012) The effects of dissolved organic matter on mercury biogeochemistry. Environmental Chemistry and Toxicology of Mercury. Wiley, 259–92, New York

Gilmour C, Bell JT, Soren AB, Riedel G, Riedel G, Kopec AD, Bodaly RA (2018) Distribution and biogeochemical controls on net methylmercury production in Penobscot River marshes and sediment. Sci Total Environ 640:555–569. https://doi.org/10.1016/j.scitotenv.2018.05.276

He RS, Xu RH, Wei CH (2015) Spectral characterization of dissolved organic matter in bio-treated effluent of coking waste water. Environmental Chemistry. 1: 129– 36. https://doi.org/10.7524/j.issn.0254-6108.2015.01.2014042401

Huang H, Mitchell CP (2023) Spatial and seasonal patterns of mercury concentrations, methylation and demethylation in central Canadian boreal soils and stream sediment. Sci Total Environ 891:164447. https://doi.org/10.1016/j.scitotenv.2023.164447

Hudelson KE, Drevnick PE, Wang F, Armstrong D, Fisk AT (2020) Mercury methylation and demethylation potentials in Arcti lake sediments. Chemosphere 248:126001. https://doi.org/10.1016/j.chemosphere.2020.126001

Jiang S, Liu X, Chen Q (2011) Distribution of total mercury and methylmercury in lake sediments in Arctic Ny-Ålesund. Chemosphere 83:1108–1116. https://doi.org/10.1016/j.chemosphere.2011.01.031

Jiang T, Bravo AG, Skyllberg U, Bjorn E, Wang D, Yan H, Green NW (2018) Influence of dissolved organic matter (DOM) characteristics on dissolved mercury (hg) species composition in sediment porewater of lakes from Southwest China. Water Res 146:146–158. https://doi.org/10.1016/j.watres.2018.08.054

Jin HJ, Yu SP, Guo D, Zhi LL, Wu LY (2006) Degradation of permafrost in the Da and Xiao Hinggan Mountains, Northeast China, and preliminary assessment of its trend. J Glaciology Geocryology 04467–476. https://doi.org/10.1016/S1001-8042(06)60011-0

Jiskra M, Wiederhold JG, Skyllberg U, Kronberg R-M, Hajdas I, Kretzschmar R (2015) Mercury Deposition and Re-emission pathways in Boreal Forest Soils Investigated with hg isotope signatures. Environ Sci Technol 49:7188–7196. https://doi.org/10.1021/acs.est.5b00742

Karhu K et al (2014) Temperature sensitivity of soil respiration rates enhanced by microbial community response. Nature 513:81–84

Li X, Ding L, Li X, Zhu Y (2020) Abundance, diversity, and structure of Geobacteraceae community in paddy soil under long-term fertilization practices. Appl Soil Ecol 153:103577. https://doi.org/10.1016/j.apsoil.2020.103577

Lin H, Morrell-Falvey JL, Rao B, Liang L, Gu B (2014) Coupled mercury–cell sorption, reduction, and oxidation on methylmercury production by Geobacter sulfurreducens PCA. Environ Sci Technol 48:11969–11976. https://doi.org/10.1021/es502537a

Liu MY (2022) Experimental study on the adsorption behavior of heavy metal Cd by humic acid and soil aggregates structure [D]. China University of Mining and Technology. https://doi.org/10.27623/d.cnki.gzkyu.2022.001018

Liu W, Chen S, Qin X, Baumann F, Scholten T, Zhou Z, Qin D, Sun W, Zhang T, Ren J (2014) Storage, patterns, and control of soil organic carbon and nitrogen in the northeastern margin of the Qinghai–Tibetan Plateau. Environ Res Lett 7:035401. https://doi.org/10.1088/1748-9326/7/3/035401

Liu YR, Dong JX, Han LL, Zheng YM, He JZ (2016) Influence of rice straw amendment on mercury methylation and nitrification in paddy soils. Environ Pollut 209:53–59. https://doi.org/10.1016/j.envpol.2015.11.023

Mailman M, Bodaly RA (2005) Total mercury, methylmercury, and carbon in fresh and burned plants and soil in Northwestern Ontario. Environ Pollut 138:161–166. https://doi.org/10.1016/j.envpol.2005.02.005

Mitchell CP, Gilmour CC (2008) Methylmercury production in a Chesapeake Bay salt marsh. J Geophys Research: Biogeosciences 113(G2). https://doi.org/10.1029/2008JG000765

Mu C, Zhang T, Zhang X, Cao B, Peng X (2016) Sensitivity of soil organic matter decomposition to temperature at different depths in permafrost regions on the northern Qinghai-Tibet Plateau. Eur J Soil Sci 67:773–781. https://doi.org/10.1111/ejss.12386

Ouellet J-F, Lucotte M, Teisserenc R, Paquet S, Canuel R (2009) Lignin biomarkers as tracers of mercury sources in lakes water column. Biogeochemistry 94:123–140. https://doi.org/10.1007/s10533-009-9314-z

Patriarca C, Sedano Nú̃nez VT, Garcia SL, Bergquist J, Bertilsson S, Sj̈oberg PJR, Tranvik LJ, Hawkes JA (2021) Character and environmental lability of cyanobacteria-derived dissolved organic matter. Limnol Oceanogr 66:496–509. https://doi.org/10.1002/lno.11619

Piao S, Huang M, Liu Z, Wang X, Ciais P, Canadell JG, Wang K, Bastos A, Friedlingstein P, Houghton RA, Le Quéré C, Liu Y, Myneni RB, Peng S, Pongratz J, Sitch S, Yan T, Wang Y, Zhu Z, Wu D, Wang T (2018) Lower land-use emissions responsible for

increased net land carbon sink during the slow warming period. Nat Geosci 11:739–743

Ravichandran M (2004) Interactions between mercury and dissolved organic matter—a review. Chemosphere 55:319–331. https://doi.org/10.1016/j.chemosphere.2003.11.011

Schaefer JK, Rocks SS, Zheng W, Liang L, Gu B, Morel FM (2011) Active transport, substrate specificity, and methylation of hg (II) in anaerobic bacteria. Proc Natl Acad Sci 108:8714–8719. https://doi.org/10.1073/pnas.1105781108

Schaefer JK, Kronberg RM, Morel FM, Skyllberg U (2014) Detection of a key hg methylation gene, hgcA, in wetland soils. Environ Microbiol Rep 6:441–447. https://doi.org/10.1111/1758-2229.12136

Schuster PF, Schaefer KM, Aiken GR et al (2018) Permafrost stores a globally significant amount of mercury. Geophys Res Lett 45:1463–1471. https://doi.org/10.1002/2017GL075571

Selin NE (2009) Global biogeochemical cycling of mercury: a review. Annu Rev Environ Resour 34:43–63. https://doi.org/10.1146/annurev.environ.051308.084314

Shao D, Kang Y, Wu S, Wong MH (2012) Effects of sulfate reducing bacteria and sulfate concentrations on mercury methylation in freshwater sediments. Sci Total Environ 424:331–336. https://doi.org/10.1016/j.scitotenv.2011.09.042

Skyllberg U, Qian J, Frech W, Xia K, Bleam WF (2003) Distribution of mercury, methyl mercury and organic sulphur species in soil, soil solution and stream of a boreal forest catchment. Biogeochemistry 64:53–76. https://doi.org/10.1023/A:1024904502633

Sun S, Kang S, Huang J, Chen S, Zhang Q, Guo J, Liu W, Neupane B, Qin D (2017) Distribution and variation of mercury in frozen soils of a high-altitude permafrost region on the northeastern margin of the Tibetan Plateau. Environ Sci Pollut Res 24:15078–15088. https://doi.org/10.1007/s11356-017-9088-0

Tomiyasu T, Nagano A, Sakamoto H, Yonehara N (2020) Background levels of atmospheric mercury in Kagoshima City, and influence of mercury emission from Sakurajima Volcano, Southern Kyushu, Japan. Sci Total Environ 259:231–237. https://doi.org/10.1016/S0048-9697(00)00585-4

Ullrich SM, Tanton TW, Abdrashitova SA (2001) Mercury in the aquatic environment: a review of factors affecting methylation. Crit Rev Environ Sci Technol 31:241–293. https://doi.org/10.1080/20016491089226

Vriens B, Lenz M, Charlet L, Berg M, Winkel LH (2014) Natural wetland emissions of methylated trace elements. Nat Commun 5:3035. https://doi.org/10.1038/ncomms4035

Wang X, Lin C-J, Lu Z, Zhang H, Zhang Y, Feng X (2016) Enhanced accumulation and storage of mercury on subtropical evergreen forest floor: implications on mercury budget in global forest ecosystems. J Geophys Res-Biogeo 121:2096–2109. https://doi.org/10.1002/2016JG003446

Wang X, Yuan W, Feng X, Wang D, Luo J (2019a) Moss facilitating mercury, lead and cadmium enhanced accumulation in organic soils over glacial erratic at Mt. Gongga, China. Environ Pollut 254:112974. https://doi.org/10.1016/j.envpol.2019.112974

Wang X, Yuan W, Lin CJ, Zhang L, Zhang H, Feng X (2019b) Climate and vegetation as primary drivers for global mercury storage in surface soil. Environ Sci Technol 53:10665–10675. https://doi.org/10.1021/acs.est.9b02386

Wang J, Shaheen SM, Jing M, Anderson CW, Swertz AC, Wang SL, Feng X, Rinklebe J (2021) Mobilization, methylation, and demethylation of mercury in a paddy soil under systematic redox changes. Environ Sci Technol 55:10133–10141. https://doi.org/10.1021/acs.est.0c07321

Wang Y, Liu J, Liem-Nguyen V, Tian S, Zhang S, Wang D, Jiang T (2022) Binding strength of mercury (II) to different dissolved organic matter: the roles of DOM properties and sources. Sci Total Environ 807:150979. https://doi.org/10.1016/j.scitotenv.2021.150979

Wei X, Zhu Z, Liu Y et al (2020) C: N: P stoichiometry regulates soil organic carbon mineralization and concomitant shifts in microbial community composition in paddy soil. Biol Fertil Soils 56:1093–1107. https://doi.org/10.1007/s00374-020-01468-7

Xin Y, Zhang X, Zhang D, Zhang Z, Jiang M (2023) Impacts of spectral characteristics of dissolved organic matter on methylmercury contents in peatlands, Northeast China. Environ Geochem Health 45:913–923. https://doi.org/10.1007/s10653-022-01257-1

Xue Z, Jiang M, Zhang Z, Wu H, Zhang T (2021) Simulating potential impacts of climate changes on distribution pattern and carbon storage function of high-latitude wetland plant communities in the Xing'anling mountains, China. Land Degrad Dev 32:2704–2714. https://doi.org/10.1002/ldr.3945

Yang Z, Fang W, Lu X, Sheng GP, Graham DE, Liang L, Gu B (2016) Warming increases methylmercury production in an Arctic soil. Environ Pollut 214:504–509. https://doi.org/10.1016/j.envpol.2016.04.069

Zhang Z, Li M, Li Z, Xue Z, Jiang M (2020) Unexpected high methylmercury contents related to soil organic carbon and its molecular composition in wetland soils of the Yarlung Tsangbo River, Tibet. Geoderma 377:114607. https://doi.org/10.1016/j.geoderma.2020.114607